GeoAmericas2020
4th PAN AMERICAN CONFERENCE ON GEOSYNTHETICS
26-29 APRIL 2020 • RIO DE JANEIRO • BRAZIL

Evaluation of the Shape of the Distribution of the Maximum Reinforcement Load in Reinforced Soil Walls

S.H. Mirmoradi, Department of Civil Engineering, COPPE, Federal University of Rio de Janeiro, UFRJ, Rio de Janeiro, Brazil, email address: shm@ufrj.br.
M. Ehrlich, Department of Civil Engineering, COPPE, Federal University of Rio de Janeiro, UFRJ, Rio de Janeiro, Brazil, email address: me@coc.ufrj.br.

ABSTRACT
This study numerically investigates the combined effect of different controlling factors on the shape of the distribution of the maximum reinforcement load, T_{max}, in reinforced soil walls (RSWs) under working stress conditions. The numerical study carried out using PLAXIS was first validated against data from wrapped and block reinforced soil walls built at Federal University of Rio de Janeiro, COPPE/UFRJ and the Royal Military College of Canada (RMC), respectively. The parametric study was then performed considering different factors such as reinforcement and facing stiffness, wall height, compaction-induced stress, foundation conditions and toe resistance. The results of the parametric study show that the shape of the distribution of the reinforcement load may be a function of the combined effect of the mentioned controlling factors considered in the current study. For a given facing stiffness with toe restriction, increasing the height of the wall and reinforcement stiffness may change the distribution shape of the reinforcement load from trapezoidal to the triangular. The importance of the toe restriction on the distribution shape of the reinforcement load may be highly influenced by the wall height. For a short wall with high toe restriction, the shape of the T_{max} with depth is trapezoidal. Moreover, the compaction-induced stress may significantly affect the distribution shape of T_{max} depending on the magnitude of the compaction effort and wall height.

1. INTRODUCTION

Today, reinforced soil walls (RSWs) are widely used around the world as earth retaining walls, and these structures must be both internally and externally stable. For external stability, the analysis of reinforced soil structures can be performed using the same methods as for traditional earth-retaining structures. For internal stability, sufficient reinforcement should be provided to avoid reinforcement rupture and pullout of the reinforcement from the anchorage zone. It should be also guaranteed to prevent connection failure between the reinforcement layers and the wall facing. Regarding internal design of RSWs, the most important aspect is the prediction of the maximum reinforcement load, T_{max}.

Several design methods have been presented and used for T_{max} determination that are based on limit equilibrium procedures (e.g. AASHTO 2017). Although these methods are very simple to use, they have some important drawbacks. In these methods, the effects of reinforcement deformability, soil deformability, compaction, and in some cases cohesion, are simply disregarded (Ehrlich and Becker, 2010; Mirmoradi and Ehrlich, 2015a). Working stress design methods have been developed to address more realistic approaches to the complex behavior of reinforced soil structures (e.g. Ehrlich and Mitchell, 1994; Allen and Bathurst 2015; Liu, 2015). In the actual field conditions, the wall may be far from failure. The determined T_{max} under working stress conditions may be significantly different from the corresponding value under soil failure conditions.

Current design methods assume different shape of the distribution of T_{max} with depth below the wall top. Typical distributions of T_{max} with depth below the wall top are triangular (e.g., Tie back wedge method, Bell et al. 1975), semi-triangular (e.g., AASHTO Simplified Method, Ehrlich and Mitchell 1994, Ehrlich and Mirmoradi 2016, Ehrlich et al. 2017), trapezoidal (e.g., K-stiffness, Bathurst et al. 2008), and rectangular (e.g., Borms 1978). The present study numerically investigates the combined effect of different controlling factors on the shape of the distribution of T_{max} RSWs under working stress conditions.

2. MODEL VALIDATION

Plane-strain numerical modelling was performed using PLAXIS 8 (Brinkgreve and Vermeer 2002). The numerical model was first validated against data from two physical models of RSWs with wrapped and block facings. The wrapped-face wall

was validated against the results of a large-scale wrapped reinforced soil wall constructed at the Geotechnical Laboratory of COPPE/UFRJ (Ehrlich and Mirmoradi 2013), while the block-face wall was validated against data from a full-scale physical model RSW built at the Royal Military College of Canada (RMC) (Hatami and Bathurst 2005).

A comparison of the results shows good general agreement between the measured and calculated values of the reinforcement load, the horizontal facing displacement, and the vertical and horizontal toe reactions during all stages of wall construction. Ehrlich and Mirmoradi (2013) and Mirmoradi and Ehrlich (2015a,b) give details of the validation of these numerical analyses, including the material properties, interfaces and boundary conditions, stage construction, compaction simulation and comparison of results.

3. PARAMETRIC STUDY

Parametric studies were carried out with different combinations of wall height, backfill soil compaction efforts, reinforcement stiffness, toe and foundation conditions, and facing type and stiffness. The following three different wall heights, H, were considered: 4, 8, and 16 m. The length and vertical spacing of the reinforcements were 0.8H and 0.4 m, respectively. The facing type was evaluated considering wrapped and block facing with vertical inclination. The block facing considering two different stiffness modulus values was evaluated. The backfill soil compaction was simulated using the procedure recommended by Mirmoradi and Ehrlich (2014b, 2015b, 2018). In this procedure, the compaction-induced stress is modeled by applying an equal distribution load at the top and bottom of the entire surface of each soil layer. Three different compaction conditions were considered in the analyses, i.e., without compaction, 63 kPa, and 120 kPa. Two different foundation stiffnesses were used in the parametric study: $0.1E_{fill}$, and $1.0E_{fill}$. Furthermore, to investigate the influence of toe restriction on the T_{max} distribution, two extreme toe conditions, fixed and free, were used. Besides that, excavation near to the toe of the wall was modelled at 1 m and 2 m depths, as shown in Figure 1.

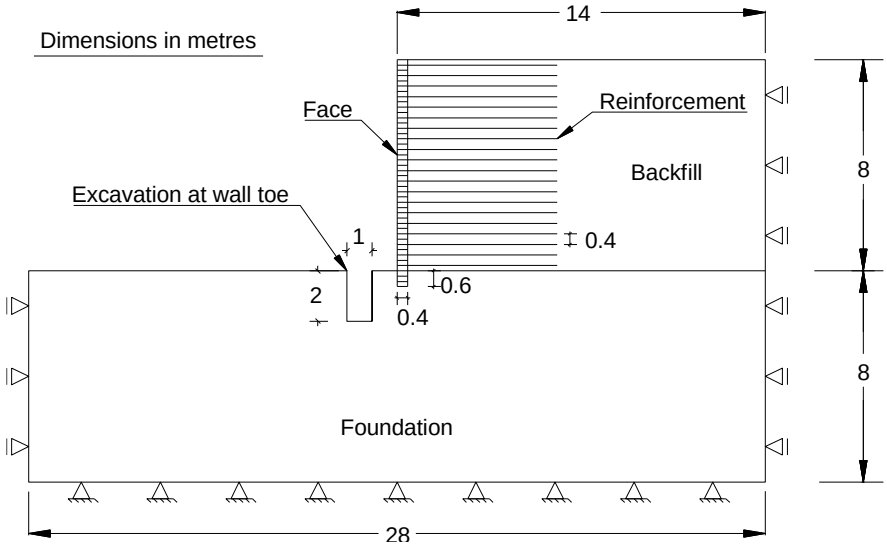

Figure 1. Typical numerical model.

The backfill was modelled using the Hardening Soil (HS) model. Hyperbolic stress-strain curves were adjusted to fit measurements from the laboratory plane-strain tests reported by Ehrlich and Mirmoradi (2013) and Hatami and Bathurst (2005). The reinforcement was modelled as a linear-elastic material with perfect interface adherence to the adjacent soil, which is a reasonable assumption for a soil-reinforcement interface under working stress conditions (Jewell 1980; Dyer and Milligan 1984; Ehrlich and Mitchell 1994; Hatami and Bathurst 2005; Mirmoradi and Ehrlich 2015a,b). Different values of the tensile stiffness modulus of reinforcement, J_r, were employed in the calculations representing typical values for the conventional polymeric and steel reinforcements used in RSWs. The values for the relative soil-reinforcement stiffness index, S_i, of 0.013, 0.025, 0.25, 1.3, and 2.5 were determined based on the reinforcement stiffnesses considered in the analyses. The parameter S_i was developed by Ehrlich and Mitchell (1994), and can be calculated as follows:

$$S_i = J_r / kP_aS_v \quad [1]$$

where J_r is the tensile stiffness modulus of reinforcement, k is Duncan et al.'s (1980) modulus number for loading (hyperbolic stress-strain curve model), P_a is the atmospheric pressure, and S_v is the vertical reinforcement spacing.

Triangular elements with 15 nodes were used to model the soil layers and other volume clusters, and a fine mesh was used to divide the system into discrete segments for study. A fixed boundary condition was employed in the horizontal direction at the right lateral border. At the base of the model, a fixed boundary condition in both the horizontal and vertical directions was applied. Fig. 1 shows the geometry of a wall with a height of 8 m. Table 1 presents the input parameters used for the backfill, facing and interfaces in the parametric study.

Table 1. Input parameters for the parametric study.

Property	Value
Facing	
type	Block, wrapped
Model	Linear elastic
Unit weight, γ (kN/m^3)	22
Poisson's ratio, υ	0.15
Stiffness modulus (GPa)	1, 10
Soil properties	
Model	Hardening soil
Peak plane strain friction angle, ϕ (º)	44, 50
Cohesion, c (kPa)	1.0
Dilation angle, Ψ (º)	0, 11
Unit weight, γ (kN/m^3)	16.8, 20
E_{50}^{ref}, (MPa)	43, 57
E_{ur}^{ref}, (MPa)	127, 170
Stress dependence exponent, m	0.5
Failure ratio, R_f	0.9
Poisson's ratio, υ	0.25
Block-block interface	
Friction angle, ϕ (º)	57
Cohesion, (kPa)	46
Soil-block interface	
Friction angle, ϕ (º)	44
Cohesion (kPa)	1
Dilation angle, Ψ (º)	11
Foundation	
Unit weight, γ (kN/m^3)	16
Cohesion, c (kPa)	20
Peak plane strain friction angle, ϕ (º)	44
Poisson's ratio, υ	0.3
E_{50}^{ref} (MN/m²)	5.7, 57
E_{ur}^{ref} (MN/m²)	17, 170
Stress dependence exponent, m	0.5
Reference pressure, P_{ref} (kN/m²)	100
Failure ratio, R_f	0.9

4. RESULTS AND DISCUSSION

Figure 2 shows the normalized values of maximum reinforcement load, T_{max}, versus elevation for the models with 4 m and 8 m heights, for wrapped and block facings. The figure shows that for walls with different facing types, the influence of the facing on the magnitude of the maximum reinforcement load decrease with wall height. For the 4 m-high wall, when the block face is modelled, the maximum reinforcement load is influenced by the stiffness of the block facing almost over the entire wall height, and has values lower than the corresponding K_a line except for the top reinforcement layer. When the wrapped face is employed, the maximum loads in the reinforcement layers are well represented by the K_a line up to a certain depth, and this is followed by a decrease in the layers located near the foundation due to the influence of foundation restriction on the reinforcement load mobilisation.

For the 8 m-high wall, T_{max} at the upper mid-height of the walls is practically the same, and is well represented by the K_a line (almost 3 m above the base of the wall) for both block- and wrapped-face walls. Below this 3 m height, however, a higher reduction in the maximum loads in the reinforcements is observed for the block facing than for the wrapped facing, due to the combined effects of facing stiffness and toe restriction. These results agree with the results of the physical and numerical modeling found in the literature (e.g., Mirmoradi et al. (2016, 2019).

Figure 3 compare the normalized values of the distribution of the maximum reinforcement load for different wall height and facing stiffness values for the fixed-base condition and Si of 0.25. The figure shows that the combined effect of the wall height and the facing stiffness for the fixed-toe conditions on the distribution of the maximum reinforcement load may be limited to about 4 m above the wall base. For the 8 m- and 16m-high walls, this effect is limited to around 50% and 25% of the wall height, respectively. For the 4 m-high wall, however, this combined effect influenced the reinforcement load in almost all of the reinforcement layers. Furthermore, for walls with fixed base conditions, the shape of the distribution of the reinforcement load varies with wall height. In a 4 m-high wall, this shape may be more trapezoidal with the maximum T_{max} at the mid-height of the wall. For the taller wall, however, the shape of the distribution of the reinforcement load may be triangular with the maximum T_{max} closer to the bottom of the wall. These findings are supported by the relative facing stiffness index, EI/γH5, as presented by Mirmoradi and Ehrlich (2015a), which significantly decreases for tall walls.

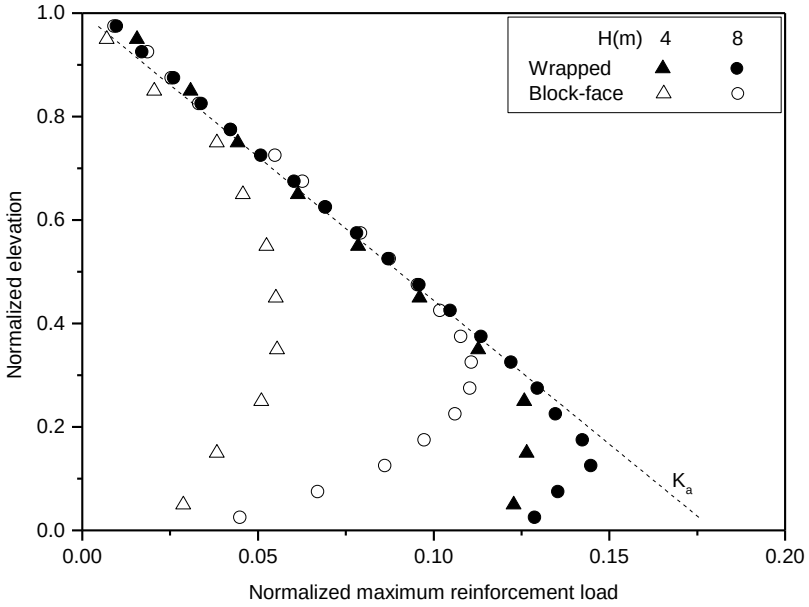

Figure 2. Relation between the normalized elevation and maximum reinforcement loads for different wall height and facing types.

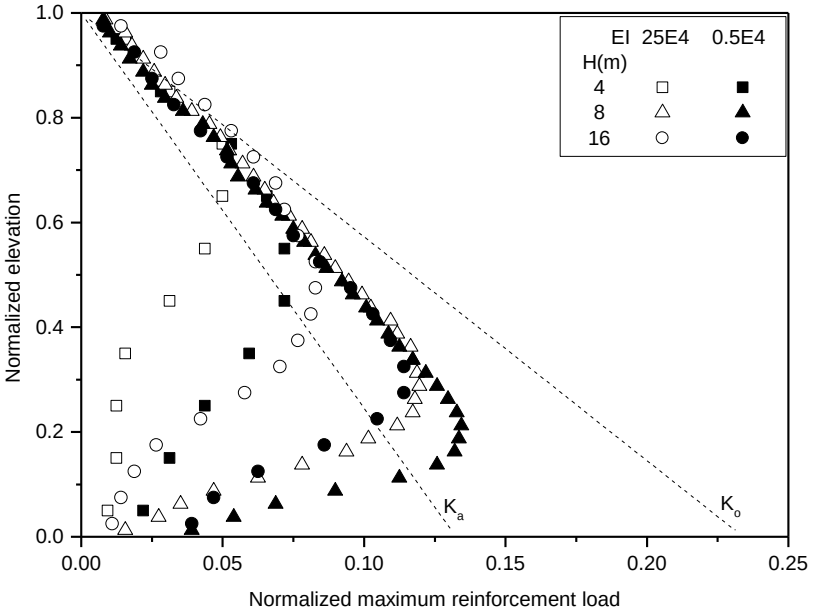

Figure 3. Relation between the normalized elevation and maximum reinforcement load for different wall height and facing stiffness (Si = 0.25).

Figure 4 compare the normalized values of the distribution of the maximum reinforcement load for different wall heights and reinforcement stiffness for the fixed-base conditions. The figure indicates that for a given wall height, decreasing the reinforcement stiffness leads to more uniform distribution of the reinforcement load with depth. This is consistent with the results presented by Ho and Rowe (1992). This also implies that increasing S_i results in changes the shape of the distribution of the reinforcement load from trapezoidal to triangular. Note that the triangular shape of distribution is more pronounced for taller walls, as previously discussed. The triangular shape distribution has also been observed in previous numerical and field investigations for a tall wall with high S_i values (e.g., Runser et al., 2001; Stuedlein et al., 2012; Mirmoradi and Ehrlich, 2017). Furthermore, there is not a significant difference between the reinforcement load for different S_i values near the wall top, as shown in previous studies (e.g., Rowe and Ho, 1993; Ehrlich and Mitchell, 1994).

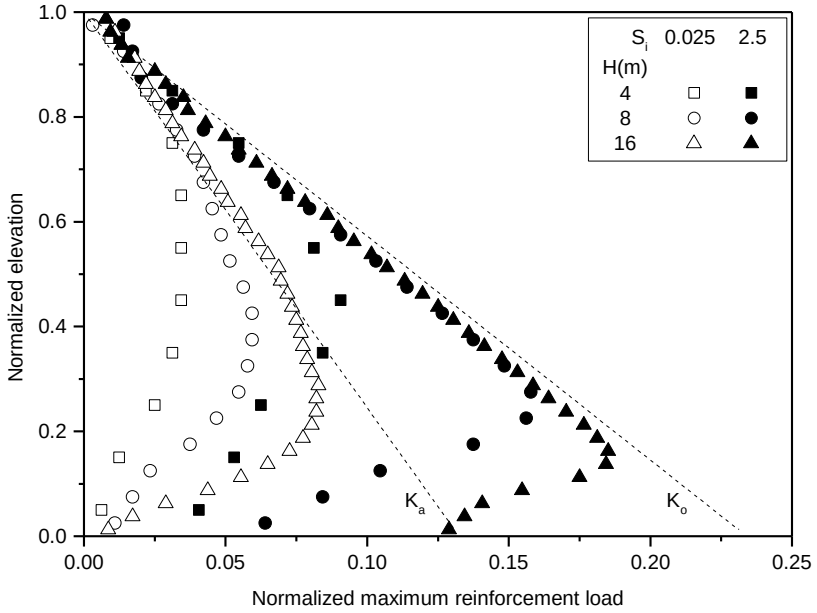

Figure 4. Relation between the normalized elevation and maximum reinforcement load for different wall height and reinforcement stiffness.

Figure 5 shows the variation in the reinforcement load as a function of wall height for the fixed and free-base conditions for 4 m, 8 m, and 16 m walls for S_i equal to 0.025. The figure shows that the combined effect of the facing stiffness and toe resistance on the magnitude of the reinforcement load may be limited to the bottom of the walls (i.e. less than 4 m from the base of the wall regardless of the wall height). Figure 5 illustrates an increase in the reinforcement load at the bottom of the wall, in which the base of the face is free. It should be noted that the fixed-base and free-base conditions are the upper and lower bounds of the possible conditions found in the field.

Figure 6 shows the normalized values of the reinforcement loads for the model with an 8 m-high block-faced wall and E_f=E_b for excavation at the toe of the wall for S_i of 0.013 and 1.3. The results indicate that due to the excavation near the toe of the wall, the load in the reinforcement placed close to the base of the wall increases, and the shape of the distribution of the T_{max} with wall height may be better represented by a triangular rather than a trapezoidal shape. This is in agreement with the previous studies have demonstrated that a yielding foundation can cause an increase in the lateral displacement of the wall facing and the reinforcement load in layers placed near the base of the wall (e.g. Schmertmann et al. 1989, Palmeria and Monte 1997, Rowe and Skinner 2001). As stated by Mirmoradi and Ehrlich (2014a, 2015a, 2016), "the practice of ignoring the toe restraint produced by a 0.3–0.5 m-deep block may be justified in the design, to increase the margin of safety against reinforcement overstressing in the case where lateral movements of the toe blocks occur." This also agrees with the discussions presented by Leshchinsky and Tatsuoka (2013), Leshchinsky et al. (2014) and Tatsuoka et al. (2014).

Figure 7 illustrates the normalized values of the distribution of T_{max} for different wall heights and foundation stiffnesses for S_i = 0.013. The results show that the position of the maximum T_{max} depends on the foundation conditions. For the block-faced wall, the effect of the foundation conditions on the maximum reinforcement loads is limited to a height of about 3 m above the bottom of the wall. This means that the relative importance of the influence of the foundations on the mobilised maximum reinforcement loads decreases with the height of the wall. Figure 7 also illustrates that for conventional polymeric reinforcement (S_i = 0.025), depending on the foundation stiffness, the maximum reinforcement loads coincide with the

corresponding K_a line above a height of 2.5–4 m from the bottom of the wall, and that this range depends on the foundation stiffness.

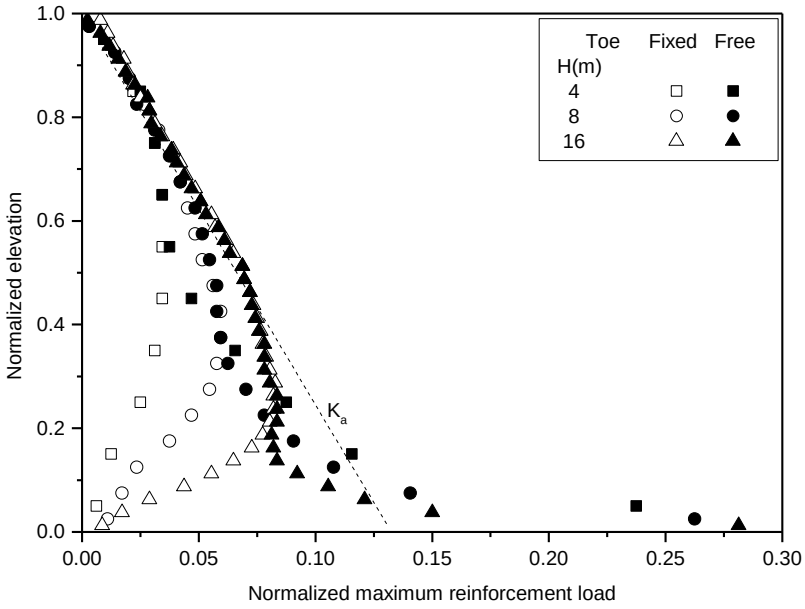

Figure 5. Relation between the normalized elevation and maximum reinforcement load for different wall height and toe conditions (S_i = 0.025).

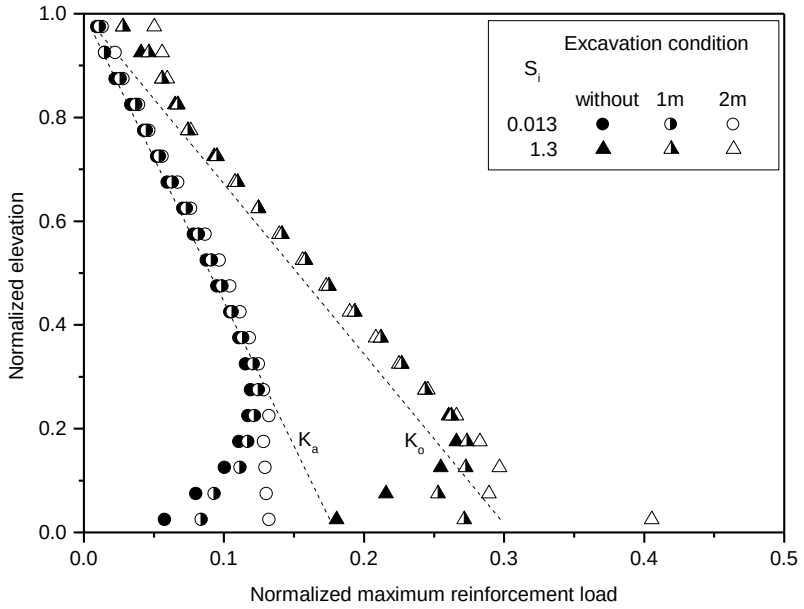

Figure 6. Relation between the normalized elevation and maximum reinforcement loads for different excavation conditions near the toe.

However, for the reinforcement in this zone, the maximum reinforcement load reaches a minimum value in the reinforcement layer placed at the bottom of the wall, due to the effects of the foundation on the lateral restriction at the bottom of the wall. This coincides with the results presented by Ho and Rowe (1992), Rowe and Ho (1993), Holtz and Lee (2002). Liu and Won (2009), and Jiang et al. (2019). Note that these results are irrespective of the height of the wall, and that this highlights the relative importance of the foundation conditions as a function of wall height on the behavior of RSWs.

Figure 8 shows the normalized elevation and T_{max} for different values of induced stress due to compaction, $\sigma'_{zc,i}$, (i.e., no compaction, 63 kPa, and 120 kPa) for block and wrapped faced walls. In performed analyses reinforcement stiffness index, Si, equal to 0.025 was assumed. In this analysis, the facing inclination of 8º to the vertical was used.

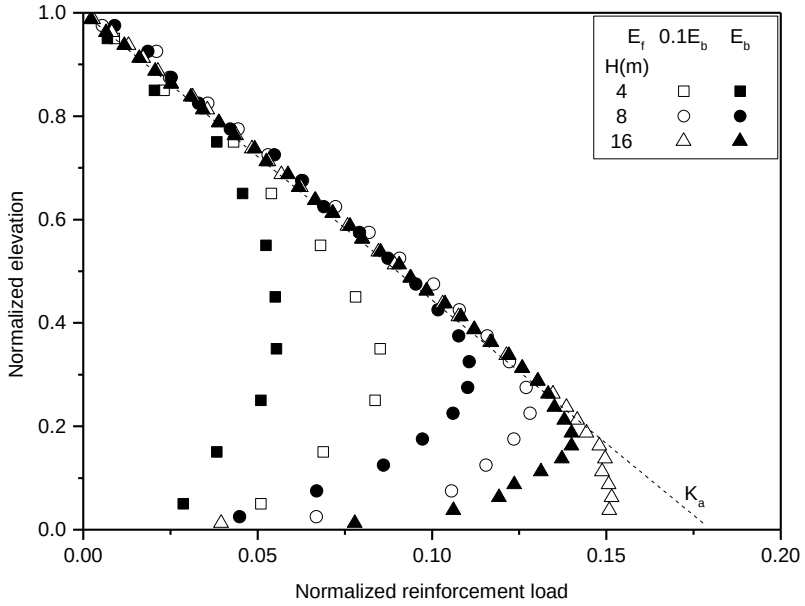

Figure 7. Relation between the normalized elevation and maximum reinforcement loads for different wall height and foundation stiffnesses.

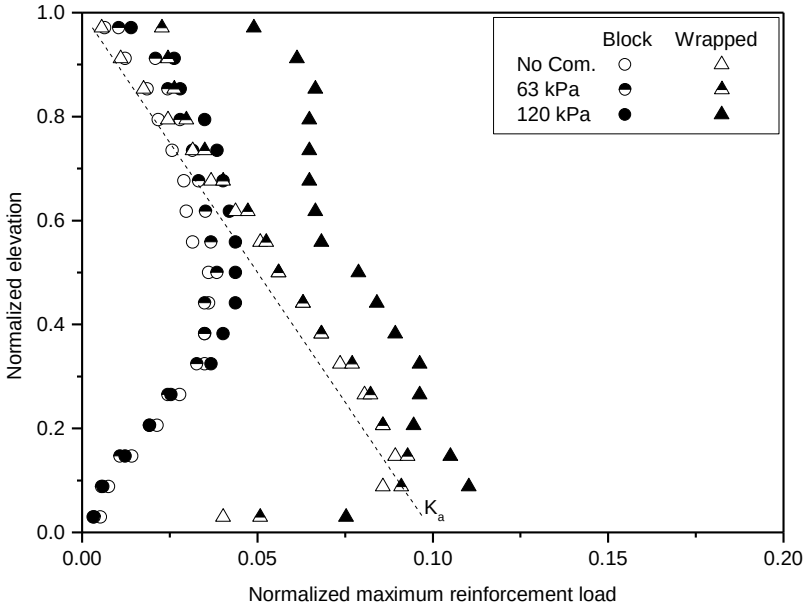

Figure 8. Relation between the normalized elevation and maximum reinforcement load for different compaction conditions.

Comparison of the curves related to the results considering or not considering the induced stress due to compaction shows a consistent representation of the expected behavior for block and wrapped faced walls. For a depth greater than the compaction influence depth, Z_c, the effect of compaction vanishes because the geostatic stress overcomes the induced stress due to the backfill soil compaction and T_{max} for the analyzes considering or not considering the induced stress due to backfill soil compaction would be the same. Z_c is given by $\sigma'_{zc,i}$ divided by the soil unit weight ($\sigma'_{zc,i}/\gamma$). However, for depths lower than the compaction influence depth ($Z < Z_c$), T_{max} would be greater than the corresponding values for the

condition of no compaction. This behavior is verified in both models with different facing types. These results agree with the reported physical modeling results by Ehrlich et al. (2012), which evaluated the effect of compaction on the behavior of GRS walls.

In addition, Figure 8 indicates that the shape of the distribution of T_{max} depends on the combined effect of the compaction effort factor, CF, facing stiffness and toe resistance and may be trapezoidal, triangular our rectangular. The parameter CF was defined by Mirmoradi and Ehrlich (2015a), as follows:

$$CF = \sigma'_{zc,i} / \gamma H \quad [2]$$

5. CONCLUSIONS

This study has numerically investigated the combined effects of different design factors (i.e. foundation condition, wall height, reinforcement stiffness, facing type and stiffness, toe resistance and compaction induced stress) on the shape of the distribution of the maximum reinforcement load, T_{max}, in reinforced soil walls, RSWs, under working stress conditions. Numerical modelling was first validated against measured data from a full-scale RSW constructed at the Geotechnical Laboratory of COPPE/UFRJ for a wrapped-face wall, and data from the Royal Military College of Canada for the block-face wall. A comparison between the measured and calculated values shows good general agreement (Mirmoradi and Ehrlich 2015a, 2017).

The results show that the combined effect of the mentioned factors may control the shape of the distribution of the reinforcement load. For a given facing stiffness with toe restriction, increasing the height of the wall and reinforcement stiffness may change the distribution shape of the reinforcement load from trapezoidal to the triangular. Furthermore, the importance of the toe restriction on the distribution of the reinforcement load may be highly influenced by the wall height. For a short wall with high toe restriction, the shape of the T_{max} with depth is trapezoidal. Decreasing this restriction lead to an increase of the load in the reinforcement layers placed close to the wall bottom and as a result, the shape of the distribution of T_{max} may be better represented by triangular shape. Moreover, the compaction-induced stress may significantly affect the distribution shape of T_{max} depending on the facing stiffness and toe resistance in combination with the magnitude of the compaction effort and wall height. Depending on the combined effect of these factors, the distribution of T_{max} may be trapezoidal, triangular or rectangular.

ACKNOWLEDGEMENTS

The authors are grateful for the funding for this study provided by the Brazilian Federal Agency for Support and Evaluation of Graduate Education, CAPES and the Brazilian Research Council, CNPq.

REFERENCES

AASHTO (2017). AASHTO LRFD bridge design specifications. American Association of State Highway and Transportation Officials, 8th ed. Washington, D.C., USA.

Allen, T.M., Bathurst, R.J. (2015). An improved simplified method for prediction of loads in reinforced soil walls. *ASCE J. Geotech. Geoenviron. Eng.* 141 (11): 04015049.

Bathurst, R. J., Miyata, Y., Nernheim, A., and Allen, A. M. (2008). Refinement of K-stiffness method for geosynthetic-reinforced soil walls. *Geosynth. Int.,* 15(4): 269–295.

Bell, J.R., Stilley, A.N., and Vandre, B. (1975). Fabric retained earth walls. *In Proceedings of the 13th Annual Engineering Geology and Soils Engineering Symposium*, University of Idaho, Moscow, Idaho. Idaho Department of Highways, Boise, Idaho: 271–287.

Brinkgreve, R.B.J. and Vermeer, P.A., (2002). PLAXIS: Finite Element Code for Soil and Rock Analyses. CRC Press, Balkema, Leiden, Netherlands version 8.

Broms, B.B. (1978). Design of fabric reinforced retaining structures. *In Proceedings of the Symposium on Earth Reinforcement, ASCE Annual Convention*, Pittsburg, Penn., 27 April 1978. ASCE, Pittsburgh, Pa: 282–304.

Duncan, J. M., Byrne, P., Wong, K. S. and Mabry, P. (1980). Strength, stress–strain and bulk modulus parameters for finite element analyses of stresses and movements in soil masses, *Geotechnical Engineering Research,* Report No. UCB/GT/80-O1. Berkeley, CA, USA: University of California.

Dyer, N.R. and Milligan, G.W.E. (1984). A photoelastic investigation of the interaction of a cohesionless soil with reinforcement placed at different orientations." *Proc., Int. Conf. on In-Situ Soil and Rock Reinforcement*, *International Society of Soil Mechanics and Geotechnical Engineering (ISSMGE)*, London: 257–262.

Ehrlich M, Becker LDB. (2010). Reinforced soil wall measurements and predictions. In: *9th International conference on geosynthetics*. Brazil: 9ICG; 547–559.

Ehrlich, M. and Mitchell, J.K. (1994). Working stress design method for reinforced soil walls. *J. Geot. Eng.* ASCE 120 (4): 625-645.

Ehrlich, M. and Mirmoradi, S.H. (2013). Evaluation of the effects of facing stiffness and toe resistance on the behavior of GRS walls. *J. Geotextile Geomembr*., 40: 28-36.

Ehrlich, M. and Mirmoradi, S.H. (2016). A simplified working stress design method for reinforced soil walls. *Geotechnique*, 66 (10): 854–863.

Ehrlich, M., Mirmoradi, S.H., and Saramago, R.P. (2012). Evaluation of the effect of compaction on the behavior of geosynthetic-reinforced soil walls. *J. Geotextile Geomembr*., 34(Oct): 108–115.

Ehrlich, M., Mirmoradi, S.H. and Xu D.S. (2017). A simplified working stress design method for reinforced soil walls. *Geotechnique*, 67 (11): 1029-1032.

Hatami, K. and Bathurst, R.J., (2005). Development and verification of a numerical model for the analysis of geosynthetic reinforced-soil segmental walls*. Can. Geotech. J.* 42 (4): 1066-1085.

Holtz, R.D. and Lee, W.F. (2002). Internal Stability Analyses of Geosynthetic Reinforced Retaining Walls. In: Final Research Report No. WA-RD 532.1, Washington State Department of Transportation.

Ho, S.K. and Rowe, R.K. (1992). Finite element analysis of geosynthetic reinforced soil walls. To appear in *Geosynthetic 93 conference*, Vancouver.

Jewell, R.A. (1980). *Some effects of reinforcement on the mechanical behavior of soils*. Ph.D. thesis, Univ. of Cambridge, Cambridge, U.K.

Jiang, Y., Han, J., Zornberg, J., Parsons, R.L., Leshchinsky, D. and Tanyu, B. (2019). Numerical Analysis of Field Geosynthetic-Reinforced Retaining Walls with Secondary Reinforcement. *Geotechnique*, 69(2): 122-132.

Leshchinsky, D., Kang, B., Han, J. and Ling, H. (2014). Framework for Limit State Design of Geosynthetic-Reinforced Walls and Slopes. *Transportation Infrastructure Geotechnology*. 1(2): 129-164.

Leshchinsky, D. and Tatsuoka, F. (2013). Geosynthetic reinforced walls in the public sector: performance, design, and redundancy. *Geosynth. Mag.*, 31(3): 12–21.

Liu, H. and Won, M.S. (2009). Long-term reinforcement load of geosynthetic-reinforced soil retaining walls. *J. Geotech. Geoenviron. Eng. ASCE*, 135 (7): 875-889.

Liu, H. (2015). Reinforcement load and compression of reinforcedsoil mass under surcharge loading. *J. Geotech. Geoenviron. Engng, ASCE* 141(6): 04015017.

Mirmoradi, S.H. and Ehrlich, M. (2014a). Geosynthetic Reinforced Soil Walls: Experimental and Numerical Evaluation of the Combined Effects of Facing Stiffness and Toe Resistance on Performance. Proc., *10th Int. Conf. on Geosynthetics, International Society of Soil Mechanics and Geotechnical Engineering (ISSMGE)*, Berlin, Germany.

Mirmoradi, S.H., Ehrlich, M. (2014b). Modeling of the compaction-induced stresses in numerical analyses of GRS walls. *Int. J. Comput. Methods*, Special Issue "Comput. Geomech."11 (2): 14.

Mirmoradi, S.H. and Ehrlich, M. (2015a). Numerical Evaluation of the Behavior of GRS Walls with Segmental Block Facing under Working Stress Conditions. *ASCE J. Geotech. Geoenviron. Eng.,* 141 (3): 04014109.

Mirmoradi, S.H. and Ehrlich, M. (2015b). Modeling of the Compaction-induced Stress on Reinforced Soil Walls. . Geotextile Geomembr. 43 (1): 82-88.

Mirmoradi, S.H. and Ehrlich, M. (2016). Evaluation of the effect of toe restraint on GRS walls. *Transportation Geotechnics, SI: Geosynthetics in Tpt,* 8: 35–44.

Mirmoradi, S.H., Ehrlich, M., and Dieguez, C. (2016). Evaluation of the Combined Effect of Toe Resistance and Facing Inclination on the Behavior of GRS Walls. *J. Geotextile Geomembr*., 44(3): 287–294.

Mirmoradi, S.H. and Ehrlich, M. (2017). Effects of facing, reinforcement stiffness, toe resistance, and height on reinforced walls. *J. Geotextile Geomembr*. 45 (1): 67–76.

Mirmoradi, S. H. and Ehrlich, M. (2018). Numerical simulation of compaction-induced stress for the analysis of RS walls under working conditions. *J. Geotextile Geomembr.*, 46: 354–365.

Mirmoradi, S.H., Ehrlich, M., Chinchay, P. and Dieguez, C. (2019). Evaluation of the combined effect of facing inclination and uniform surcharge on GRS walls. *J. Geotextile Geomembr*. 103485.

Palmeria, E.M. and Monte, L.M. (1997). The behaviour of model reinforced walls on soft soils. *Geosynthetics '97,* Long Beach California, USA, 11–13 March 1997. Industrial Fabrics Association International: 73–84.

Rowe, R.K. and Ho, S.K., (1993). Keynote lecture: A review of the behavior of reinforced soil walls. Earth Reinforcement Practice, Proc. *Int. Symposium on Earth Reinforcement Practice*, Vol. 2, Kyushu University, Fukuoka, Japan, November 1992, H. Ochiai, S. Hayashi, and J. Otani, eds., Balkema, Rotterdam, The Netherlands: 801– 830.

Rowe, R.K, Skinner, G.D. (2001). Numerical analysis of geosynthetic reinforced retaining wall constructed on a layered soil foundation. *J Geotext Geomembr*,19(7): 387–412.

Runser, D.J., Fox, P.J., and Bourdeau, P.L. (2001). Field Performance of a 17 m-High Reinforced Soil Retaining Wall, *Geosynthetics International*, 8(5): 367-391.

Stuedlein, A.W., Allen, T.M., Holtz, R.D. and Christopher, B.R. (2012). Assessment of Reinforcement Strains in Very Tall Mechanically Stabilized Earth Walls. *ASCE J. Geotech. Geoenviron. Eng.,* 138 (3): 345-456.

Schmertmann, G.R., Chew, S.H., Mitchell, J.K. (1989). Finite element modelling of reinforced soil wall behaviour. Department of Civil Engineering, University of California, Berkeley, *Geotechnical Engineering Report* UCB/GT/89-01.

Tatsuoka, F., Koseki, J. and Kuwano, J. (2014). Natural disasters mitigation by using construction methods with geosynthetics (earthquakes). Keynote Lecture, *10th international conference on geosynthetics,* Berlin, ISSMGE, 53p.